Thermochimica Acta 520 (2011) 145–152

Contents lists available at ScienceDirect

Thermochimica Acta

journal homepage: www.elsevier.com/locate/tca

Studies on fluorination of Y_2O_3 by NH_4HF_2

Abhishek Mukherjee [a], Alok Awasthi [a,*], Saurabh Mishra [b], Nagaiyar Krishnamurthy [a]

[a] Materials Processing Division, Bhabha Atomic Research Centre, Mumbai 400085, India
[b] Department of Metallurgical Engineering and Materials Science, Indian Institute of Technology Bombay, Mumbai 400076, India

ARTICLE INFO

Article history:
Received 16 October 2010
Received in revised form 30 March 2011
Accepted 31 March 2011
Available online 12 April 2011

Keywords:
Ammonium yttrium fluorides
Rare earth fluoride
Fluorination

ABSTRACT

Fluorination of Y_2O_3 by NH_4HF_2 to obtain pure YF_3 is studied in this work by observing the mass changes at room temperature and by employing TGA and DTA at higher temperatures, and observing the subsequent phase changes by X-ray diffraction. Fluorination begins at room temperature with the formation of $(NH_4)_3Y_2F_9$ and NH_4F, and continues with the later further fluorinating any leftover Y_2O_3 to ammonium yttrium fluorides with the evolution of NH_3. Similarly, on heating a mixture of Y_2O_3 and NH_4HF_2, the reaction proceeds sequentially through the formation of $(NH_4)_3Y_2F_9$, $NH_4Y_2F_7$ and finally YF_3. Any Y_2O_3 still remaining reacts with YF_3 to form yttrium oxyfluorides, which continue as impurity. Substantial evaporation of NH_4HF_2 is possible even before it could participate in the reaction. This disturbs the stoichiometry of the charge causing oxygen to remain in final YF_3. The compound reported in literature as $YF_3{\cdot}1.5NH_3$ appears to be $NH_4Y_2F_7$.

1. Introduction

Metallothermic reduction of rare-earth oxides results in rare-earths which contain substantial amount of oxygen [1]. Fluorides are therefore used for the preparation of rare-earths with less oxygen. Rare-earth fluorides are non-hygroscopic and are therefore preferred over cheaper chlorides. Rare earths are highly reactive and their preparation has to be done in an oxygen-free inert atmosphere. If oxygen purity of the starting fluoride could be ensured besides maintaining the inert atmosphere, then its reduction should result in a purer rare-earth product.

Fluorination of rare earth oxides can be done using fluorine gas (F_2) [2,3], hydrogen fluoride gas (HF) [4], aqueous hydrofluoric acid (HF) [5], ammonium fluoride (NH_4F) or ammonium hydrogen fluoride (NH_4HF_2). Of these, fluorine and hydrogen fluoride are corrosive and poisonous gases and thus are difficult to handle. Moreover, there remains a possibility of unreacted oxide remaining in the product [2,6], at least during the static-bed fluorination carried out using these gases. Aqueous hydrofluoric acid is again highly corrosive. NH_4F is highly hygroscopic. Contact of water vapour and rare-earth fluoride has to be avoided, as there remains a possibility of oxygen contamination due to pyrohydrolysis of the fluoride [7,8]. Fluorination of the oxide by NH_4HF_2 therefore appears to be the most convenient method for obtaining oxygen-free fluoride. The preparation of oxygen-free YF_3 by the reaction of Y_2O_3 with NH_4HF_2 is studied in this work. There is no evidence to suggest solubility of oxygen in YF_3 and the absence of yttrium oxyfluorides in the product has been considered sufficient to term YF_3 as oxygen-free.

It is known in the literature [5,6] that the fluorination of rare earth oxides by NH_4HF_2 occurs as per the following overall reaction (1) at temperatures about 300 °C. To ensure complete fluorination, 30% excess NH_4HF_2 is used than the stoichiometric amount.

$$Y_2O_3 + 6NH_4HF_2 = 2YF_3 + 6NH_4F + 3H_2O \quad (1)$$

NH_4F, H_2O and excess NH_4HF_2 evaporate at these temperatures and thus only YF_3 remains in the solid form.

Kalinnikov et al. [9] have recently studied the changes occurring on heating a mixture of NH_4HF_2 and Y_2O_3 in 4.5:1 ratio by thermal analysis techniques and have found that the fluorination proceeds through two ammonium yttrium fluorides, $(NH_4)_3Y_2F_9$ and $NH_4Y_2F_7$. In the present work, the effects of varying the NH_4HF_2 content of the charge have been studied. The occurrence of fluorination at room temperature is also examined in detail. Attempts are made to identify the factors, which could lead to oxygen remaining in the product during scale-up.

Besides being used for fluorinating rare earth oxides, NH_4HF_2 has also been employed for fluorination of ZrO_2 [10–12], BeO [13], Sr_2CuO_3 [14], UO_2 [15], ThO_2 [16], V_2O_3 [17] etc., and the methodologies adopted in the present work may be useful for optimizing the process parameters for these oxides as well, at least during the dry processing.

* Corresponding author. Tel.: +91 22 25595111; fax: +91 22 25505151.
E-mail address: aawasthi@barc.gov.in (A. Awasthi).

0040-6031/$ – see front matter © 2011 Elsevier B.V. All rights reserved.
doi:10.1016/j.tca.2011.03.032

2. Experimental

Yttrium oxide (Y_2O_3) powder used in this work was of 99.9% purity. Commercial grade (97% pure) crystals of ammonium bifluoride (NH_4HF_2) and ammonium fluoride (NH_4F) were used. Isolated compounds $(NH_4)_3Y_2F_9$ and $NH_4Y_2F_7$ used further in the experiments were made by heating the mixtures of NH_4HF_2 and Y_2O_3 in at least 7.5:1 mole ratio at temperatures 275–375 °C for sufficient duration in argon flow and confirming the products by mass change and X-ray diffraction.

Samples of NH_4HF_2 and Y_2O_3 were prepared by mixing the compounds together in the required ratio until the mixture visually appeared uniform. The mixtures have been designated according to their stoichiometry. For example, a mixture containing NH_4HF_2 and Y_2O_3 in 3:1 mole ratio is termed $3NH_4HF_2 + Y_2O_3$ mixture. A few mixtures were kept at room temperature for varying durations in plastic bags. Most of the mixtures were treated at high temperatures.

Simultaneous thermogravimetric analysis (TGA) – differential thermal analysis (DTA) curves for NH_4HF_2 and a few mixtures of Y_2O_3 and NH_4HF_2 were generated in a commercial unit (model SDT Q800 of TA Instruments make) with about 10 mg charge heated at 10 °C/min rate in a platinum cup under nitrogen flow (100 ml/min for NH_4HF_2 and NH_4F, and 50 ml/min for the mixtures) and with alumina as the reference material. The simultaneous TGA–DTA unit was available only for some experiments. Further experiments were carried out in a home-made DTA unit with about 0.5 g charge in static air atmosphere in a vitreous silica cup with alumina as the reference. The rate of heating was nominally kept 10 °C/min in the home-made unit, although the unit had an initial thermal inertia, due to which the increase in temperature upto 70 °C was slower and non-linear. Some of the runs carried out in the home-made DTA unit were stopped after specific DTA events and the phases present in such products were analysed.

Phase identification was carried out by X-ray diffraction (XRD) in an Inel-make unit (model MPD) with Cu-$K_{\alpha 1}$ radiation at 30 mA 40 kV using a curved position-sensitive detector, thereby observing the diffraction data in complete 2θ range of interest simultaneously. The XRD unit was equipped with parabolic mirrors to enhance the intensity of the X-ray beam. The samples were spinned during the XRD analysis around the vertical axis, thereby eliminating diffraction effects due to orientation in r and θ directions. A satisfactory XRD pattern could be recorded in this unit in 3–4 min.

3. Results and discussion

3.1. Reactions at room temperature

All the samples became reasonably warm during mixing of the powders, alluding to the occurrence of an exothermic chemical reaction even at room temperature. Another interesting observation was made in a few sealed bags containing the samples. After placing the samples, these bags were completely deflated to remove the air inside and the seals were closed. Some of the bags became inflated after some time, thereby indicating that the reaction had a gaseous product. Smell of ammonia could be observed from some of the bags.

Appreciable mass changes were also observed with time even at room temperature (Fig. 1), which are possible only if a gas or vapour is absorbed or desorbed from the samples. The masses of the samples with NH_4HF_2:Y_2O_3 mole ratio of less than 4.5 initially fast decrease and then become constant with time. However, sample $6.5NH_4HF_2 + Y_2O_3$ shows increase in mass.

The samples were analysed by XRD (Fig. 2) after being kept at room temperature for about 360 h as indicated by the final points in Fig. 1. Table 1 shows the phases identified by XRD in these old samples and the corresponding changes in the mass. Presence of ammonium yttrium fluorides in these samples confirmed the occurrence of a chemical reaction at the room temperature.

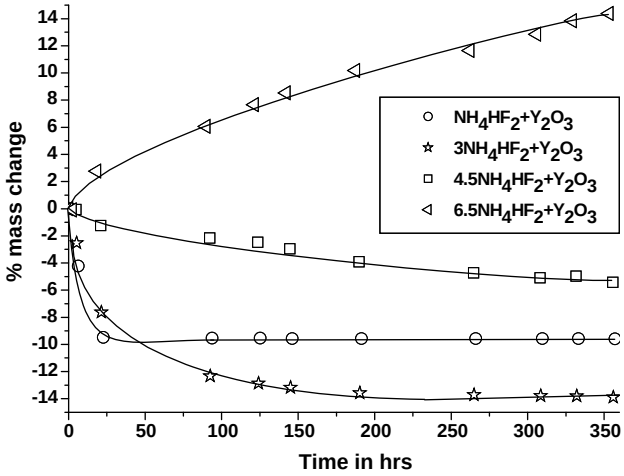

Fig. 1. Mass changes observed in various samples at room temperature with time.

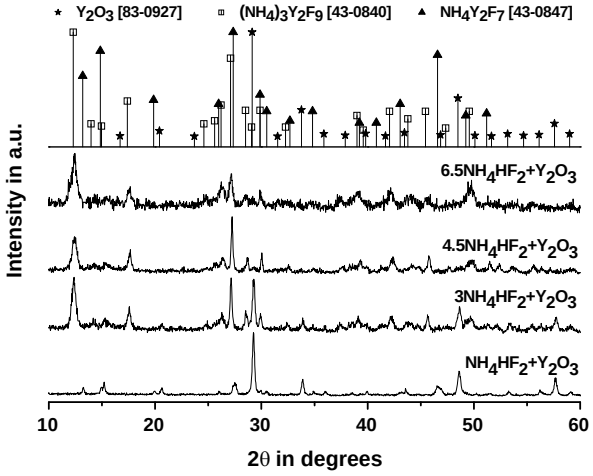

Fig. 2. XRD of samples of various compositions after being kept at room temperature for about 360 h (exact duration is indicated by the final points in Fig. 1).

However, the relative intensities of some of the peaks of $(NH_4)_3Y_2F_9$ were not constant in these samples (Fig. 2). Examination of the isolated compounds using scanning electron microscope indicated that, unlike $NH_4Y_2F_7$ and Y_2O_3, the particles of $(NH_4)_3Y_2F_9$ apparently had a long needle-like structure. In the presence of H_2O, they probably oriented themselves in a preferred way in the z-direction while placing the sample on the XRD holder. The effects of preferred orientation in z-direction could not be eliminated by spinning and these apparently caused the variation in the peak heights of $(NH_4)_3Y_2F_9$.

Table 1
The mass changes and the phases observed in the mixtures of NH_4HF_2 and Y_2O_3 when kept at room temperature for about 360 h after mixing.

Sample	% Mass change when XRD was carried out	Phases identified by XRD (Fig. 2)
$NH_4HF_2 + Y_2O_3$	−9.6	$NH_4Y_2F_7$, Y_2O_3
$3\ NH_4HF_2 + Y_2O_3$	−13.9	$(NH_4)_3Y_2F_9$, Y_2O_3
$4.5\ NH_4HF_2 + Y_2O_3$	−5.4	$(NH_4)_3Y_2F_9$
$6.5\ NH_4HF_2 + Y_2O_3$	14.4	$(NH_4)_3Y_2F_9$

If material balance for the following reaction (2) is considered,

$$7NH_4HF_2 + 2Y_2O_3 = 2NH_4Y_2F_7 + 6H_2O_{(vapour)} + 5NH_3 \quad (2)$$

the mass loss on complete consumption of NH_4HF_2 present in the sample of $NH_4HF_2 + Y_2O_3$ should be 9.7%. It is reasonable to consider H_2O in vapour form, as the duration of the experiment is long enough to indeed allow its evaporation. Similarly, the mass loss for the reaction (3)

$$9NH_4HF_2 + 2Y_2O_3 = 2(NH_4)_3Y_2F_9 + 6H_2O_{(vapour)} + 3NH_3 \quad (3)$$

in samples $3NH_4HF_2 + Y_2O_3$ and $4.5NH_4HF_2 + Y_2O_3$ should be 13.4 and 34.5% respectively. The observed mass losses and the XRD data (Figs. 1 and 2, Table 1) are consistent with these calculations, if the occurrence of reaction (2) for sample $NH_4HF_2 + Y_2O_3$ and of reaction (3) for sample $3NH_4HF_2 + Y_2O_3$ is considered. However, the mass loss for sample $4.5NH_4HF_2 + Y_2O_3$ was substantially lower, whereas sample $6.5NH_4HF_2 + Y_2O_3$ showed mass gain.

NH_4F is known to be highly hygroscopic and the reason of the mass gain may lie in this fact. The moisture pickup by NH_4F and NH_4HF_2 exposed to air was observed; those had gained 76.3% and 3.3% mass respectively in a similar duration. If the following reaction (4) occurs, then not only the product H_2O should remain in the sample, product NH_4F should also pickup moisture from air.

$$6NH_4HF_2 + Y_2O_3 = (NH_4)_3Y_2F_9 + 3H_2O + 3NH_4F \quad (4)$$

If the moisture pickup data by the product NH_4F and also by the remaining NH_4HF_2 (in case of sample $6.5NH_4HF_2 + Y_2O_3$) is considered, samples $4.5NH_4HF_2 + Y_2O_3$ and $6.5NH_4HF_2 + Y_2O_3$ should gain 13.6% and 14.4% mass respectively on completion of reaction (4). The observed mass change in $4.5NH_4HF_2 + Y_2O_3$ sample was in between the calculated mass changes for reactions (3) and (4), so probably both of these reactions occurred in this sample. Similarly, the mass gain data for sample $6.5NH_4HF_2 + Y_2O_3$ matches with the calculated data for reaction (4), thereby indicating the occurrence of this reaction. Also, the XRD data is noisier for this sample (Fig. 2), apparently due to Compton scattering because of the presence of H_2O [18].

However, neither the excess reactant NH_4HF_2 nor the product NH_4F was detected in the presence of yttrium compounds by XRD (Table 1, Fig. 2). Yttrium atom due to its substantially higher atomic number (Z) scatters X-rays very strongly as compared to hydrogen, nitrogen or fluorine atoms [18], and therefore the peaks of yttrium containing compounds in XRD are substantially stronger than those of the compounds of low-Z atoms like NH_4HF_2 and NH_4F. XRD of a mixture of NH_4HF_2 and $(NH_4)_3Y_2F_9$ in as high a mole ratio as 9:5 was recorded; no peaks of NH_4HF_2 were observed.

It could thus be concluded that NH_4HF_2 reacts with Y_2O_3 even at room temperature to form ammonium yttrium fluorides with NH_4F and H_2O as the products. NH_4F too is not stable in the presence of Y_2O_3. If Y_2O_3 unreacted with NH_4HF_2 remains and NH_4F is also present in a sample, then following reaction (5) also occurs. Reactions (4) and (5) combine to give overall reaction (3).

$$9NH_4F + Y_2O_3 = (NH_4)_3Y_2F_9 + 3H_2O + 6NH_3 \quad (5)$$

To further confirm that NH_4F too reacts with Y_2O_3 even at room temperature, a mixture of NH_4F and Y_2O_3 in 6:1 mole ratio was made and analysed by XRD after being kept at room temperature for some time. The XRD showed $(NH_4)_3Y_2F_9$ peaks apart from Y_2O_3 peaks.

The occurrence of a reaction between Y_2O_3 and NH_4HF_2 at room temperature was reported by Patwe et al. [19]. However, they had identified the product as $(NH_4)_3YF_6{\cdot}1.5H_2O$, having the same XRD pattern, due to being isostructural, as that of $(NH_4)_3LaF_6{\cdot}1.5H_2O$. However, neither this yttrium compound was confirmed by the subsequent researchers, nor the XRD patterns recorded in the present work indicate its presence. Room temperature reactions with NH_4HF_2 resulting in ammonium metallo-fluorides have recently been reported for uranium oxide [15] and thorium oxide [16]. The XRD patterns of Silva et al. [16] do not show NH_4HF_2 and NH_4F in the old thorium oxide samples. However, Yeamans et al. [15] could identify unreacted NH_4HF_2 in $4.3NH_4HF_2 + UO_2$ sample after the complete reaction, which should result in $0.3NH_4HF_2 + (NH_4)_4UF_8 + 2H_2O$ at the time of XRD.

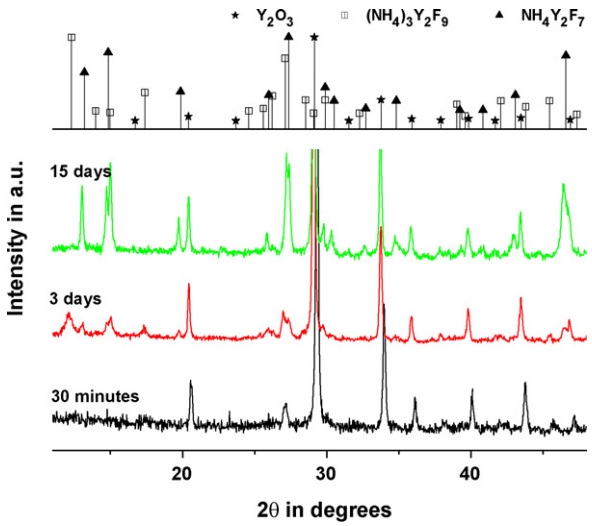

Fig. 3. Change in the XRD pattern of $NH_4HF_2 + Y_2O_3$ sample with time at room temperature indicating the formation of $(NH_4)_3Y_2F_9$ first and its conversion to $NH_4Y_2F_7$ with time.

XRD patterns of $NH_4HF_2 + Y_2O_3$ sample recorded at different times since mixing are shown in Fig. 3 and these indicate the development of phases with time in the sample. Peak of $(NH_4)_3Y_2F_9$ at 27.10° appeared within 30 min of sample preparation. The XRD pattern recorded after three days had all the peaks of $(NH_4)_3Y_2F_9$ and also of $NH_4Y_2F_7$ (*Note*: The occurrence of twin peaks around 15° and 27.5° in the XRD pattern of $NH_4Y_2F_7$ is discussed in Section 3.6). The peaks of $(NH_4)_3Y_2F_9$ completely disappeared in the pattern recorded after fifteen days and the peaks of $NH_4Y_2F_7$ fully developed. This indicates that $(NH_4)_3Y_2F_9$ forms first and gets subsequently converted to $NH_4Y_2F_7$ by reacting with remaining Y_2O_3 according to reaction (6). The overall reaction can still be represented by reaction (2), which in fact is the combination of reactions (3) and (6).

$$7(NH_4)_3Y_2F_9 + 2Y_2O_3 = 9NH_4Y_2F_7 + 6H_2O_{(v)} + 12NH_3 \quad (6)$$

Similarly, only $(NH_4)_3Y_2F_9$ (and not $NH_4Y_2F_7$) and Y_2O_3 were observed even in freshly-prepared and quickly-analysed samples of $3NH_4HF_2 + Y_2O_3$, $4.5NH_4HF_2 + Y_2O_3$ and $6.5NH_4HF_2 + Y_2O_3$; no $NH_4Y_2F_7$ was observed in such samples. This further confirms that $(NH_4)_3Y_2F_9$ forms earlier than $NH_4Y_2F_7$, even when the other product is NH_4F and not NH_3.

3.2. Home-made DTA unit and observing the room temperature reaction

Before discussing the results further, it may be appropriate to mention here that the sensitivity of the home-made DTA unit was inferior as compared to that of the professionally made simultaneous TGA–DTA unit. As mentioned earlier, the increase in temperature upto 70 °C was slower and non-linear in the home-made unit, whereas the temperature rise was linear right from the room temperature in the combined TGA–DTA unit. When the fluorine content of the charge was more (for example, in samples with NH_4HF_2 to Y_2O_3 mole ratio of 3:1 or more), the interac-

tion of fluorine with the quartz cups slightly influenced the DTA curves recorded in the home-made unit, as indicated by the kinks in the baselines in Fig. 4. However, the XRD patterns of the products remaining in the DTA cup were not affected, as the product of fluorination of quartz is gaseous at these temperatures. The powder collected from the cooler portions of the unit was identified as $(NH_4)_2SiF_6$, whereas the product remaining in the DTA cup did not have XRD peaks of any silicon compound.

According to thermodynamic data, YF_3 is more stable than Y_2O_3 [20]. Tischer and Burnet [2] have described the preparation of YF_3 by the reaction of Y_2O_3 with fluorine gas. This reaction should proceed through YOF and $YF_3{\cdot}6$–$4YOF$ compounds sequentially with oxygen evolution. Oxidation of yttrium fluoride or the oxyfluorides in air would therefore not be possible and thus the absence of the inert atmosphere in the home-made DTA unit should not make a difference. However, as the runs were carried out in static air in this unit, the beginning of a reaction having a gaseous product would be recorded at a higher temperature.

Fig. 4(a and b) shows the DTA curves of the freshly prepared (charged within 5 min of mixing) and the one-day old $3NH_4HF_2 + Y_2O_3$ charges obtained respectively in the home-made DTA unit. An exothermic peak appeared in the DTA of the fresh charge just above the room temperature, corresponding to the formation of $(NH_4)_3Y_2F_9$ as discussed in Section 3.1. This peak did not appear for the one-day old charge, as the formation of $(NH_4)_3Y_2F_9$ was over at room temperature by the time the DTA was recorded. Fig. 4 also indicates that a slight increase in temperature makes the kinetics of the room temperature reaction faster. A similar exothermic peak was observed by Kalinnikov et al. [9].

3.3. Investigation of high temperature events

The curves obtained by simultaneous TGA–DTA of NH_4HF_2 and NH_4F are shown in Fig. 5 and those obtained with freshly-prepared mixtures of NH_4HF_2 to Y_2O_3 mole ratios of 1–6.5 are given in Fig. 6. Differential thermogravimetry (DTG) data obtained by differentiating the TGA data has also been included in Figs. 5 and 6. A few events are seen in all the samples. However, boiling of H_2O at 100 °C is not clearly recorded in these curves (Fig. 6) as it evaporates continuously and very less amount of it is available by the time its boiling point is reached.

3.3.1. TGA–DTA curves of NH_4HF_2 and NH_4F

Melting point of NH_4HF_2 is reported as 126.5 °C [21]. The first peak in the DTA curve (Fig. 5c) of NH_4HF_2 was endothermic; it appeared at 125 °C and thus could be ascribed to melting. However, as is apparent from the TGA and the DTG curves (Fig. 5a and b), appreciable evaporation of NH_4HF_2 began even before its melting point was reached, thereby indicating that it has a high vapour pressure. The next DTA event began around 145 °C for NH_4HF_2, and led to its complete evaporation as indicated by TGA, apparently due to boiling. Similarly, the simultaneous TGA–DTA curves of NH_4F (Fig. 5) indicated its melting and boiling points to be 110 and 165 °C respectively, and its appreciable evaporation right from its melting point onwards.

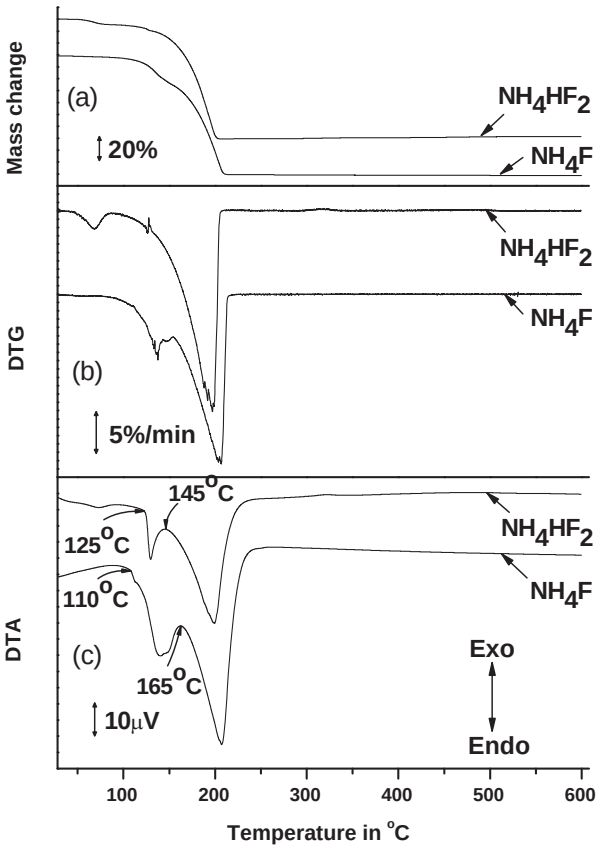

Fig. 5. Curves obtained by simultaneous TGA–DTA of NH_4HF_2 and NH_4F; (a) TGA curves (b) DTG curves and (c) DTA curves.

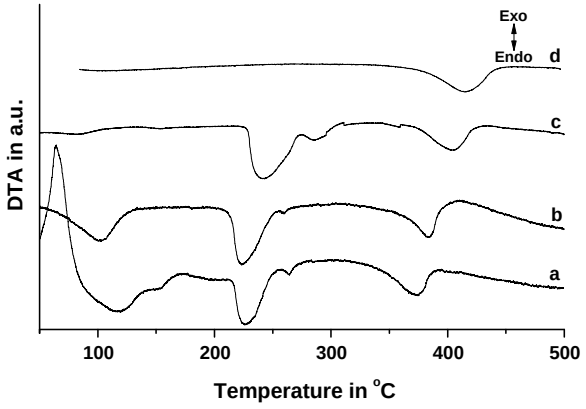

Fig. 4. DTA generated in the home-made DTA unit, (a) fresh $3NH_4HF_2 + Y_2O_3$ sample, (b) one-day old $3NH_4HF_2 + Y_2O_3$ sample, (c) $(NH_4)_3Y_2F_9$ and (d) $NH_4Y_2F_7$. The kinks in the baseline are due to interaction of quartz with fluorides of the charge.

3.3.2. Simultaneous TGA–DTA curves of mixtures–till ammonium fluorides are present

The first DTA peaks of all the samples (Fig. 6c) corresponded more or less with the melting of NH_4HF_2, considering the difference in the flowrate of the cover gas for the runs of NH_4HF_2 and the mixtures.

The second DTA peaks were exothermic. These began at the tips of the first peaks and overlapped with the third peaks as well in all the samples and thus were not very apparent. However, as observed from the DTG curves (Fig. 6b), there was an increase in the rate of mass loss when the second peaks began, and this independently confirmed the occurrence of a DTA event. Like the exothermic event observed in the DTA curve (Fig. 4) recorded in the home-made unit, the event corresponding to these exothermic peaks also appears to be the reaction of NH_4HF_2 with Y_2O_3. However, the peaks appeared at a higher temperature in the combined TGA–DTA unit as the effective rate of heating here was higher, considering the initial thermal inertia of the home-made DTA unit. Although the reaction must have begun right at the room temperature, its rate became observable only after the melting of NH_4HF_2 as the contact surface for the reaction to occur then increased. Increase in the rate of a reaction

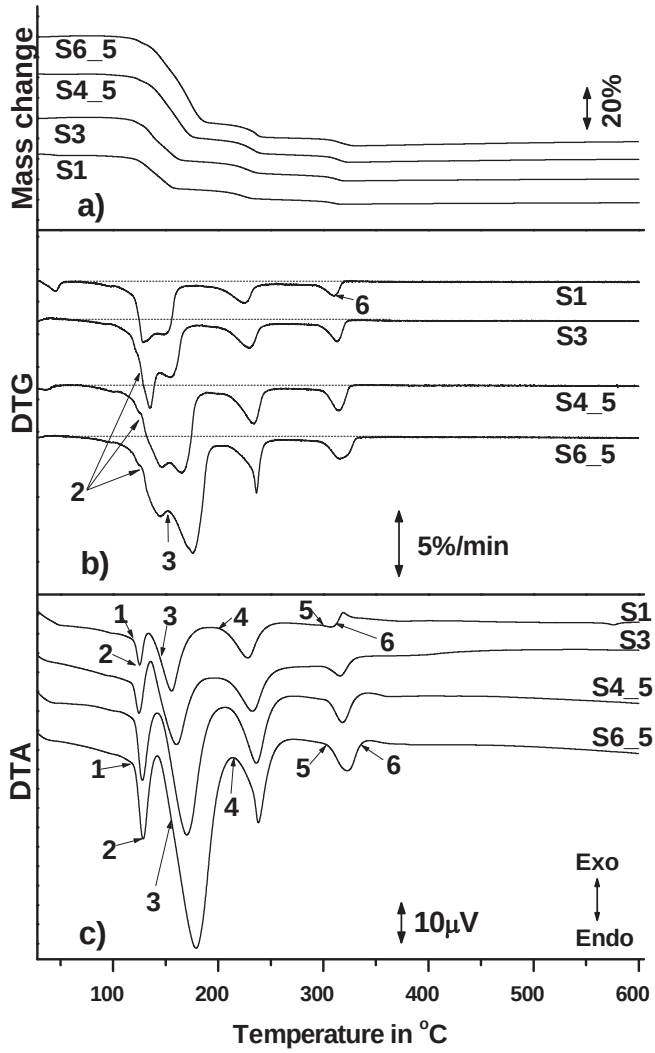

Fig. 6. Curves obtained by simultaneous TGA–DTA of freshly prepared mixtures with NH_4HF_2 to Y_2O_3 mole ratios of 1–6.5; (a) TGA curves (b) DTG curves and (c) DTA curves. Samples are indicated as per the following, S1: $NH_4HF_2 + Y_2O_3$, S3: $3NH_4HF_2 + Y_2O_3$, S4_5: $4.5NH_4HF_2 + Y_2O_3$, S6_5: $6.5NH_4HF_2 + Y_2O_3$. The beginning of the DTA events is marked by an arrow and the peak number for S1 and S6_5 as representative indication and the events for other samples can be correspondingly identified. Most of the events are identifiable on the DTG curves and not-so-apparent ones are marked there as well.

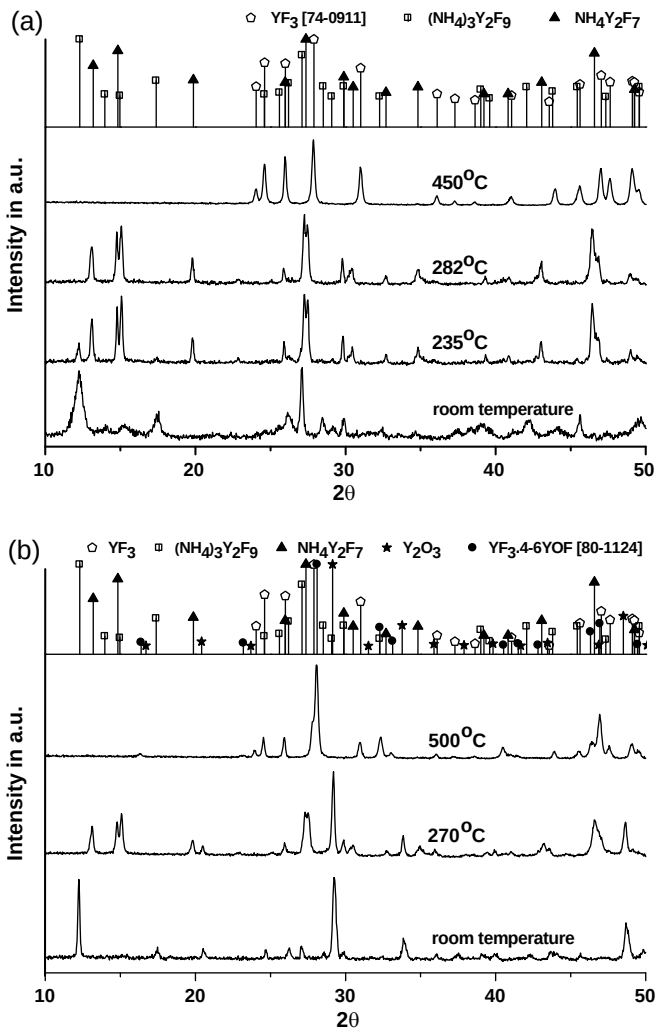

Fig. 7. XRD patterns obtained after heating (a) $7.8NH_4HF_2 + Y_2O_3$ and (b) $3NH_4HF_2 + Y_2O_3$ samples to various temperatures in home-made DTA unit. (Section 3.6 may be referred regarding the peaks of $NH_4Y_2F_7$.)

on melting of one of the reactants has been observed in other systems as well [22]. The conversion to $(NH_4)_3Y_2F_9$ is complete in the second peaks either due to the complete consumption of Y_2O_3 or of NH_4HF_2/NH_4F according to reactions (3–5).

The third DTA peaks (Fig. 6c) were endothermic and appeared around 140–155 °C to indicate the boiling of excess NH_4HF_2, if still present, and boiling of NH_4F product of reaction (4). The third peaks became appreciably bigger with NH_4HF_2 content of the starting mixture, as the amount of NH_4F forming or NH_4HF_2 remaining unreacted in the charge till this temperature was higher. This further alludes that the third peaks are not associated with any change in the yttrium compounds. As evaporation is associated with mass loss, the DTG peaks corresponding to the third DTA peaks also increased in size with NH_4HF_2 content of the charge (Fig. 6c).

When the DTA of isolated $(NH_4)_3Y_2F_9$ was recorded in the home-made DTA unit, only two peaks, occurring beyond about 200 °C, were observed (Fig. 4(c)). This is in agreement with the explanation that it is only $(NH_4)_3Y_2F_9$ which remains after the event of the third peaks.

3.3.3. *Simultaneous TGA–DTA curves of mixtures–after complete evaporation of ammonium fluorides*

To help in assessing the events occurring beyond the third peaks obtained in the simultaneous TGA–DTA unit (Fig. 6), a few samples of $7.8NH_4HF_2 + Y_2O_3$ and $3NH_4HF_2 + Y_2O_3$ compositions were heated in the home-made DTA unit to temperatures until a DTA event was crossed for each sample. The XRD pattern obtained after this heating and the maximum temperature to which the sample was heated are given in Fig. 7(a) for $7.8NH_4HF_2 + Y_2O_3$ samples and in Fig. 7(b) for $3NH_4HF_2 + Y_2O_3$ charges.

Fig. 6c indicates that the fourth DTA peaks for all the compositions were over around 260 °C. The product obtained after heating $7.8NH_4HF_2 + Y_2O_3$ sample upto 282 °C was $NH_4Y_2F_7$ (Fig. 7a), whereas a mixture of $NH_4Y_2F_7$ and excess Y_2O_3 was obtained on heating $3NH_4HF_2 + Y_2O_3$ sample upto 270 °C (Fig. 7b). Thus, the event corresponding to the fourth peak could be the complete decomposition of $(NH_4)_3Y_2F_9$ to $NH_4Y_2F_7$ according to the following reaction (7).

$$(NH_4)_3Y_2F_9 = NH_4Y_2F_7 + 2(NH_3 + HF) \quad (7)$$

It is not clear whether the evaporating species is NH_4F or a mixture of NH_3 and HF gases at reaction temperatures; it is therefore indicated as $(NH_3 + HF)$ in reaction (7) and further discussions. A comment on its nature is made in Section 3.3.4. The peak-begin

temperature of the fourth peak varied between 200 and 215 °C and increased with the NH_4HF_2 content of the starting charge. Apparently, the onset of the reaction was delayed till the vapours generated due to the evaporation of excess NH_4HF_2 left the reaction zone.

As the temperature was increased further, two events appeared to be occurring, one endothermic (fifth peaks) and the other exothermic (sixth peaks) (Fig. 6c). The endothermic DTA peaks were prominent when the charge had more NH_4HF_2. The peak was not very apparent in the case of $NH_4HF_2 + Y_2O_3$ charge. The exothermic events followed the endothermic peaks. The exothermic event was distinct in the case of $NH_4HF_2 + Y_2O_3$ charge, and appeared as a broad peak of less height for the other charges.

When the DTA of isolated $NH_4Y_2F_7$ recorded in the home-made DTA unit (Fig. 4d), only one endothermic peak appeared around 350 °C and the product was analysed as YF_3. The fifth DTA peaks were endothermic and appeared around 305 °C (Fig. 6c) and, therefore, could be assigned to the decomposition of $NH_4Y_2F_7$ of the charge (Fig. 7a and b) to YF_3 according to reaction (8).

$$NH_4Y_2F_7 = 2YF_3 + (NH_3 + HF) \quad (8)$$

The sixth and exothermic peaks appear to be occurring due to the reaction between YF_3 and the remaining Y_2O_3 (Fig. 7b) to form yttrium oxyfluorides $YF_3{\cdot}xY_2O_3$ (corresponding to YOF or $YF_3{\cdot}$4–6YOF) according to reaction (9).

$$YF_3 + xY_2O_3 = YF_3{\cdot}xY_2O_3 \quad (9)$$

Since reaction (9) is a solid-state reaction, the formation of yttrium oxyfluorides was slow, as indicated by the broad DTA peaks. This reaction (9) does not involve a mass change and therefore no corresponding change on the DTG curves was observed for all the samples but $NH_4HF_2 + Y_2O_3$. In case of $NH_4HF_2 + Y_2O_3$ charge, reaction (9) began even before the decomposition of $NH_4Y_2F_7$ was complete apparently due to a substantially higher amount of Y_2O_3 being present in the sample. It may be noted here that, thermodynamically, $NH_4Y_2F_7$ and Y_2O_3 should react to directly form $YF_3{\cdot}xY_2O_3$ at a temperature lower than the temperature required for $NH_4Y_2F_7$ decomposition to YF_3. However, the kinetics of YF_3 formation appears to be much faster in comparison to that of the direct formation of oxyfluorides, as is apparent from the occurrence of the two identifiable DTA peaks (fifth and sixth). It may be repeated here that Y_2O_3 can remain even in stoichiometric samples due to the evaporation of NH_4HF_2 and this apparently caused the small sixth peaks even in samples with higher NH_4HF_2 content (Fig. 6). In their work, Kowalczyk et al. [23] have assigned the final exothermic peak to the conversion of $YF_3{\cdot}1.5NH_3$ (actually $NH_4Y_2F_7$ as discussed in Section 3.6) to YF_3. They apparently have not considered the hyperstoichiometry of yttrium oxide resulting in the charge due to the higher evaporation of the fluorinating agent as a result of different rates of heating employed.

3.3.4. Identity of (NH_3 + HF) and its removal at lower temperature

After the runs of heating 7.5–9$NH_4HF_2 + Y_2O_3$ charges at scores of gram level at 275–375 °C were over, substantial amount of condensate was found at cooler portions of the setup. Product YF_3 remained in the hot zone of the setup, whereas excess NH_4HF_2 and product (NH_3 + HF) evaporated away and condensed in the cooler parts. This condensate was analysed to be $NH_4HF_2 + NH_4F$ mixture by XRD. This still does not prove that the evaporating species of reactions (7) and (8) are indeed NH_3 and HF gases, but even if they are, it is certain that they convert and condense to NH_4F on cooling.

When there is no mass change in a sample, the value of DTG should be observed as zero. Horizontal lines have been drawn in the DTG curves in Fig. 6b corresponding to the zero values. It is observed that prior to the beginning of the fourth and the fifth peaks, although the DTG curves became horizontal, they did not reach the zero value. This indicates that the equilibrium pressures of (NH_3 + HF) in reactions (7) and (8) were not negligible even before the beginning of these peaks. In accordance with Le Chatelier's principle, the reactions could slowly proceed rightwards even at temperatures lower than that indicated by the DTA. Holding $(NH_4)_3Y_2F_9$ at 185 °C for 4 h in the home-made DTA unit could indeed yield a mixture of $(NH_4)_3Y_2F_9$ and $NH_4Y_2F_7$. It is known in the literature [5,6] that reaction (1) is carried out at 300 °C and takes about 12 h to complete. However, for achieving faster reaction rates, it is better to have a temperature higher than the peak-begin temperature, so that the pressure of (NH_3 + HF) is more than one atmosphere.

Wang et al. [24] have reported the formation of nano-sized YF_3 of various shapes at room temperature by treating yttrium nitrate with NH_4F or NH_4HF_2 and cleaning the product by repeated centrifuge filtering and ultrasonic cleaning. Ammonium yttrium fluorides have been prepared by the reaction of yttrium nitrate with NH_4F [25]. Apparently, ultrasonic cleaning with water and centrifuging caused effective removal of (NH_3 + HF) leading to completion of reactions (7) and (8) at room temperature in Wang et al.'s [24] experiments.

Table 2
Products obtained on heating the mixtures of NH_4HF_2 and Y_2O_3 upto 500 °C.

Mixture composition	Products obtained
$NH_4HF_2 + Y_2O_3$	YF_3.4-6YOF, YOF, Y_2O_3
$1.4NH_4HF_2 + Y_2O_3$	YF_3.4-6YOF
$2NH_4HF_2 + Y_2O_3$	YF_3.4-6YOF
$3NH_4HF_2 + Y_2O_3$	YF_3.4-6YOF, YF_3
$4.5NH_4HF_2 + Y_2O_3$ (and more NH_4HF_2)	YF_3

3.4. Products obtained with varying amounts of NH_4HF_2 in charge

A few mixtures having different amounts of NH_4HF_2 were heated upto 500 °C and the products thus obtained were identified. The results are presented in Table 2. A part of the equilibrium ternary diagram of NH_4F-YF_3–Y_2O_3 system is constructed (Fig. 8) based on these results, which is valid upto the temperature of stability of the constituents in condensed forms. Mann and Bevan [7] could identify three compounds in with $YF_3{\cdot}$4YOF, $YF_3{\cdot}$5YOF and $YF_3{\cdot}$6YOF compositions having very similar XRD patterns. As these compounds have similar crystal lattices with differences only in ordering, these have been indicated as one compound with the composition range of $YF_3{\cdot}$4–6YOF. No indication of the existence

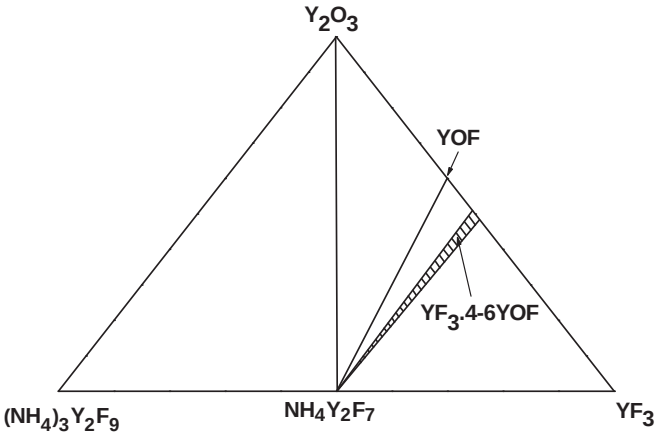

Fig. 8. A portion of the equilibrium ternary diagram of NH_4F-YF_3–Y_2O_3 system proposed from experimental observations of the present work.

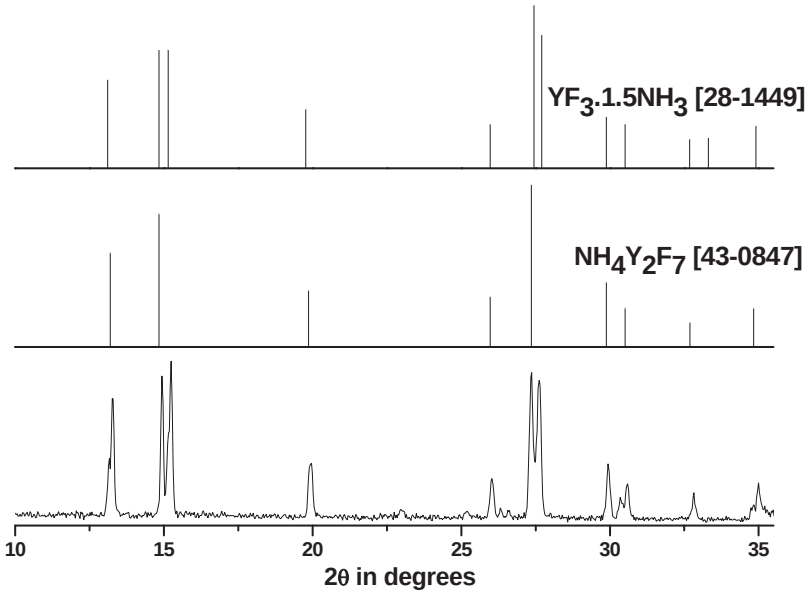

Fig. 9. XRD of the isolated $NH_4Y_2F_7$ alongwith JCPDS data on $YF_3{\cdot}1.5NH_3$ and $NH_4Y_2F_7$.

of ammonium metallo-oxyfluorides compounds like $NH_4Y_xO_yF_z$ (actually $NH_4F{\cdot}x$YOF or $NH_4F{\cdot}x(YF_3{\cdot}4–6YOF)$), which do not appear in the JCPDS data, was found for yttrium metal (Fig. 7, Table 2).

The heating of $NH_4HF_2 + Y_2O_3$ charge yielded a mixture of $YF_3{\cdot}4–6YOF$, YOF and Y_2O_3 (Table 2), although this charge is stoichiometric for YOF formation. This further indicates that the solid state reactions between yttrium oxide, oxyfluorides and fluoride are slow as compared to the formation of yttrium fluoride from ammonium yttrium fluorides (Section 3.3.3).

Similarly, $3NH_4HF_2 + Y_2O_3$ charge is stoichiometric for the formation of YF_3, if NH_3 (and not NH_4F) is the product of the fluorination reaction. However, $YF_3{\cdot}4–6YOF$ was also obtained apart from YF_3 upon heating this mixture, as some amount of NH_4HF_2 and probably also of NH_4F intermediate evaporates during heating without participating in fluorination (Section 3.3.2).

3.5. Conditions for obtaining pure yttrium fluoride

It is clear from the earlier discussions that the formation of YF_3 by fluorination of Y_2O_3 using NH_4HF_2 proceeds sequentially through reactions (4)–(8). If NH_4HF_2 content of the starting charge were sufficient to allow the complete consumption of Y_2O_3 in reaction (4) and also sufficient time were given for reaction (4) to complete, reactions (5) and (6) are omitted from this sequence. If the temperature of the charge is substantially increased before the completion of reaction (4), some NH_4HF_2 would evaporate due to its high vapour pressure leaving some Y_2O_3 unreacted, which would ultimately contaminate the final product, YF_3. Therefore, for obtaining oxygen-free YF_3, it is best to ensure the full conversion to $(NH_4)_3Y_2F_9$ and complete disappearance of Y_2O_3 at either room temperature or slightly higher temperature when the evaporation of NH_4HF_2/NH_4F is negligible. The use of excess NH_4HF_2 in the starting mixture may not be fully necessary. Once Y_2O_3 of the charge gets completely converted to $(NH_4)_3Y_2F_9$, it could then be fast heated to temperatures above 400 °C along with the use of a sweeping gas for quicker formation of YF_3. The bigger level runs for preparation of YF_3 in the present work were typically over in about 45 min at 400 °C. The exact time required for complete fluorination may substantially vary from reactor to reactor, as it would depend on the gas sweeping rate, area of the gas–solid interface, whether condensation is possible in cooler regions etc. apart from the temperature in the reaction zone.

It may now be appropriate to compare NH_4F and NH_4HF_2 as the fluorinating agents. Fluorination by NH_4F would also occur sequentially, beginning from reaction (5) and proceeding through reactions (6) if necessary, (7) and (8). Even if the formation of NH_4OH, a condensed phase, is considered by the reaction between the products NH_3 and H_2O, reaction (5) remains a solid–gas reaction, as three moles of NH_3 still remain in the gaseous form. The removal of ammonia is necessary for reaction (5) to proceed and large surface would be favourable. On the other hand, reaction (4) does not involve a gas and thus does not depend on the availability of an open surface. The dissolution of the reactant NH_4HF_2 in the product H_2O helps in its better spreading to untouched portions of Y_2O_3 due to wetting, thereby reducing the effects of the possible pockets of excess Y_2O_3 caused due to imperfect mixing. Therefore, fluorination with NH_4HF_2 should be inherently faster and more complete. No NH_3 is discharged to the atmosphere in reaction (4) and NH_4F product could be regenerated to NH_4HF_2 by reacting it with HF.

It may be appropriate to mention here that, as fluorination of yttrium oxide using NH_4F and that using NH_4HF_2, both follow the same paths reaction (5) onwards, and as the evaporation of NH_4F is substantial even before its boiling temperature, many researchers have mistakenly assigned the first endothermic peak to the decomposition of NH_4F to NH_4HF_2 and NH_3 [26–28].

3.6. Observations on the stoichiometry of ammonium yttrium fluorides

Russo and Haendler [25] have reported $(NH_4)_3Y_2F_9{\cdot}H_2O$ compound, which they prepared by reacting aqueous solutions of yttrium nitrate with NH_4F. This compound converted to $(NH_4)_3Y_2F_9$ at 92 °C. They have given the intensities of its XRD peaks qualitatively [25] [JCPDS 28-0098]. As H_2O also forms alongwith $(NH_4)_3Y_2F_9$ in reactions (3) and (4), we have considered the possibility of the formation of this hydrated compound. However, the XRD data of $(NH_4)_3Y_2F_9{\cdot}H_2O$ is similar to that of $(NH_4)_3Y_2F_9$ [JCPDS 43-0840]. It is quite probable that the variation in relative intensities of the two data was due to preferred orientation as discussed in Section 3.1 and the slight difference in *d*-spacings was due to the use of a different equipment. Reactions (3) and (4) were over by the time 92 °C was reached in DTA runs carried out in the home-made-unit (Fig. 4(a and b)); no event at this temperature was observed.

It is possible that Russo and Haendler [25] assigned the DTA event corresponding to the evaporation of free water to the dehydration of $(NH_4)_3Y_2F_9{\cdot}H_2O$.

According to JCPDS database, the XRD patterns of $NH_4Y_2F_7$ [JCPDS 43-0847] and $YF_3{\cdot}1.5NH_3$ [JCPDS 28-1449] are quite similar in *d*-spacings. Apart from the occurrence of some additional peaks of low intensity in $YF_3{\cdot}1.5NH_3$, its two highest peaks are actually twin peaks, at 0.325 and 0.322 nm (corresponding to 27.44 and 27.70° two-theta values for $CuK_{\alpha1}$) and at 0.585 and 0.597 (corresponding to 14.84 and 15.15° two-theta). The two highest peaks of $NH_4Y_2F_7$ have been reported to occur at 0.326 and 0.597 nm (corresponding to 27.36 and 14.84°) in this database. Clear twin peaks around these angles are seen in the XRD of $NH_4Y_2F_7$ in Figs. 3 and 7(a and b). XRD of the isolated $NH_4Y_2F_7$ had clear twin peaks at 14.94° and 15.25° and at 27.36° and 27.61° (Fig. 9). Heating about ten grams of this compound at 450 °C till there was no further mass change resulted in YF_3 with 12.5% mass loss, against the stoichiometric mass loss of 11.2 and 14.9% on conversion of $NH_4Y_2F_7$ and $YF_3{\cdot}1.5NH_3$ to YF_3, respectively. As there is no possibility of mass gain due to contamination or so in a carefully carried-out experiment with handling losses being still possible, this hints that the compound was indeed $NH_4Y_2F_7$ and not $YF_3{\cdot}1.5NH_3$. JCPDS data on $YF_3{\cdot}1.5NH_3$ has been quoted from Markovskii et al. [26], who obtained this compound by heating $3NH_4F + YOF$ mixture at 210 °C for 1 h and also $6NH_4F + Y_2O_3$ mixture at 220 °C for 0.5 h. JCPDS data on $NH_4Y_2F_7$ is taken from the work of Rajeshwar and Secco [29], who prepared the compound by reacting Y_2O_3 with NH_4F and decomposing the $(NH_4)_3Y_2F_9$ thus obtained. Apart from assessing its stoichiometry by material balance calculations, Rajeshwar and Secco [29] also obtained the infrared spectrum of the compound, which had characteristics of NH_4^+. It is quite possible that Markovskii et al. [26] and Rajeshwar and Secco [29] both obtained the same compound and the later missed the close adjacent peaks. In the present work, therefore, the compound is designated as $NH_4Y_2F_7$ despite the occurrence of the twin peaks, which were observable apparently due to good peak-to-noise ratio of the XRD unit resulting from the use of parabolic mirror.

4. Conclusions

1. Fluorination of Y_2O_3 with NH_4HF_2 proceeds sequentially through the formation of $(NH_4)_3Y_2F_9$, $NH_4Y_2F_7$ and finally YF_3.
2. Reaction of NH_4HF_2 with Y_2O_3 begins at room temperature with appreciable rate. $(NH_4)_3Y_2F_9$ and NH_4F form first. Like NH_4HF_2, NH_4F also is highly unstable in the presence of Y_2O_3. It further participates in the reaction right from the room temperature with the release of NH_3.

   In other words, during the reaction of NH_4HF_2 and Y_2O_3 at room temperature, $(NH_4)_3Y_2F_9$ forms together with NH_4F if sufficient NH_4HF_2 is available in the charge. Else, it forms together with NH_3.
3. The reaction between $(NH_4)_3Y_2F_9$ and Y_2O_3 is also fast enough at room temperature to allow the observable formation of $NH_4Y_2F_7$ in a couple of days.
4. NH_4HF_2 has a high vapour pressure. Its substantial evaporation before it could react with Y_2O_3 is possible during fast heating.
5. The decomposition temperatures of $(NH_4)_3Y_2F_9$ to $NH_4Y_2F_7$ and of the later to YF_3 are indicated as 200–215 °C and 305 °C by DTA. However, due to the high vapour pressure of the evaporating species, it is possible to obtain observable amounts of the decomposition products at lower temperatures after sufficient time. Completion of these reactions noticeably depends on removal of the vapours from the reaction zone.
6. If Y_2O_3 is present even after the formation of YF_3, then it finally reacts with it to form yttrium oxyfluoride (YOF or $YF_3{\cdot}4$–$6YOF$). Oxygen remains in this form as an impurity in YF_3.
7. No indication of the existence of ammonium yttrio-oxyfluorides ($NH_4Y_xO_yF_z$) was found.
8. $YF_3{\cdot}1.5NH_3$ is actually $NH_4Y_2F_7$. Also, $(NH_4)_3Y_2F_9{\cdot}H_2O$ is possibly $(NH_4)_3Y_2F_9$.
9. For obtaining oxygen-free YF_3, it is better to first ensure the complete conversion of the oxide to $(NH_4)_3Y_2F_9$. The use of excess NH_4HF_2 in the starting mixture may not be fully necessary.

References

[1] R. Pengo, P. Favaron, G. Manente, A. Cecchi, L. Pieraccini, The reduction of rare earth oxides to metal and their subsequent rolling, Nucl. Instrum. Methods Phys. Res., Sect. A 303 (1) (1991) 146–151.
[2] R.L. Tischer, G. Burnet, Preparation of yttrium fluoride using fluorine, U.S. At. Energy Comm. IS-8 (1959).
[3] R. Bougon, J. Ehretsmann, J. Portier, A. Tressaud, in: P. Hagenmuller (Ed.), Preparative Methods in Solid State Chemistry, Academic Press Inc., New York, 1972.
[4] S.W. Kwon, E.H. Kim, B.G. Ahn, J.H. Yoo, H.G. Ahn, Fluorination of metals and metal oxides by gas solid reaction, J. Ind. Eng. Chem. 8 (5) (2002) 477–482.
[5] C.K. Gupta, N. Krishnamurthy, Extractive Metallurgy of Rare Earths, CRC Press, Boca Raton, 2004.
[6] F.H. Spedding, A.H. Daane, The Rare Earths, Wiley, New York, 1961.
[7] A.W. Mann, D.J.M. Bevan, Intermediate fluorite-related phases in the Y2O3–YF3 system – examples of one-dimensional ordered intergrowth, J. Solid State Chem. 5 (1972) 410–418.
[8] J.C. Warf, W.D. Cline, R.D. Tevebaugh, Pyrohydrolysis in the determination of fluoride and other halides, Anal. Chem. 26 (1954) 342–346.
[9] V.T. Kalinnikov, D.V. Makarov, E.L. Tikhomirova, I.R. Elizarova, V.Y. Kuznetsov, Hydrofluoride synthesis of fluorides of some rare-earth elements, Russ. J. Appl. Chem. 75 (11) (2002) 1760–1764.
[10] M. Ferraris, M. Braglia, R. Chiappetta, E. Modone, G. Cocito, Different processes for the preparation of fluorozirconate glasses, Mater. Res. Bull. 25 (1990) 891–897.
[11] D.R. MacFarlane, P.J. Mineely, P.J. Newman, Synthesis of zirconium tetrafluoride using ammonium bifluoride melts, J. Non-Cryst. Solids 140 (1992) 335–339.
[12] M. Onishi, T. Kohgo, K. Amemiya, K. Nakazato, H. Kanamori, H. Yokota, Thermal and mass analyses of fluorination process with ammonium bifluoride, J. Non-Cryst. Solids 161 (1993) 10–13.
[13] A.J. Singh, Beryllium – the extraordinary metal, Min. Process. Ext. Met. Rev. 13 (1994) 177–192.
[14] B.N. Wani, S.J. Patwe, U.R.K. Rao, R.M. Kadam, M.D. Sastry, Fluorination of Sr_2CuO_3 by NH_4HF_2, Appl. Supercond. 3 (1995) 321–325.
[15] C.B. Yeamans, G.W.C. Silva, G.S. Cerefice, K.R. Czerwinski, T. Hartmann, A.K. Burrell, A.P. Sattelberger, Oxidative ammonolysis of uranium (IV) fluorides to uranium (VI) nitride, J. Nucl. Mater. 374 (2008) 75–78.
[16] G.W.C. Silva, C.B. Yeamans, G.S. Cerefice, A.P. Sattelberger, K.R. Czerwinski, Synthesis and nanoscale characterization of $(NH_4)_4ThF_8$ and ThNF, Inorg. Chem. 48 (2009) 5736–5746.
[17] C.K. Gupta, N. Krishnamurthy, Extractive Metallurgy of Vanadium, Elsevier Science Publishers B.V., Amsterdam, 1992.
[18] B.D. Cullity, Elements of X-ray Diffraction, second ed., Addison-Wesley Publishing Company Inc., Massachusetts, 1978.
[19] S.J. Patwe, B.N. Wani, U.R.K. Rao, K.S. Venkateswarlu, Synthesis and thermal study of tris (ammonium) hexafluoro metallates (III) of some rare earths, Can. J. Chem. 67 (1989) 1815–1818.
[20] I. Barin, Thermodynamic Data of Pure Substances, third ed., VCH Verlagsgeserschaft mbH, Weinheim, 1995.
[21] J.E. House Jr., C.S. Rippon, A TG study of the decomposition of ammonium fluoride and ammonium bifluoride, Thermochim. Acta 47 (1981) 213–216.
[22] A. Awasthi, Y.J. Bhatt, N. Krishnamurthy, Y. Ueda, S.P. Garg, The reduction of niobium and tantalum pentoxides by silicon in vacuum, J. Alloys Compd. 315 (2001) 187–192.
[23] E.E. Kowalczyk, R. Diduszko, Z. Kowalczyk, T. Leszczyfiski, Studies on the reaction of ammonium fluoride with lithium carbonate and yttrium oxide, Thermochim. Acta 265 (1995) 189–195.
[24] M. Wang, Q. Huang, J. Hong, X. Chen, Controlled synthesis of different morphological YF3 crystalline particles at room temperature, Mater. Lett. 61 (2007) 1960–1963.
[25] R.C. Russo, H.M. Haendler, Ammonium fluorolanthanates, J. Inorg. Nucl. Chem. 36 (1974) 763–770.
[26] L.Y. Markovskii, E.Y. Pesina, Y.A. Omel'chenko, Thermogravimetric study of the reaction of lanthanum and yttrium oxides with ammonium fluoride, Russ. J. Inorg. Chem. 16 (1971) 172–175.
[27] J. Hölsä, L. Niinistö, Thermoanalytical study on the reactions of selected rare earth oxides with ammonium halides, Thermochim. Acta 37 (1980) 155–160.
[28] E.G. Rakov, E.I. Mel'nichenko, The properties and reactions of ammonium fluorides, Russ. Chem. Rev. 53 (1984) 851–869.
[29] K. Rajeshwar, E.A. Secco, Ammonium fluorolanthanates: solid state synthesis, infrared spectral and X-ray diffraction data, Can. J. Chem. 55 (1977) 2620–2627.